Global modelling of microinstabilities in stellarators and with electromagnetic effects using XGC

M. D. J. Cole, R. Hager, A. Mishchenko, T. Moritaka, S. H. Ku, C. S. Chang

Outline

- Introduction
- Stellarator XGC
- Explicit electromagnetic XGC
- Summary and outlook

Outline

- Introduction
- Stellarator XGC
- Explicit electromagnetic XGC
- Summary and outlook

Introduction: gyrokinetics for stellarators

- Gyrokinetics is a successful model for understanding transport in fusion plasmas, e.g. microturbulence and neoclassical driven.
- Stellarator plasmas can be turbulent, and turbulence is observed to dominate transport in optimized stellarators -> one need for stellarator gyrokinetics.
- Edge physics is important for both tokamaks and stellarators, but few codes have been able to model it -> XGC was created for this purpose.
- Stellarator edge physics presents additional challenges, e.g. islands and stochastic regions.
- Gyrokinetic code XGC has been extended for stellarator physics.

Introduction: explicit electromagnetics

- The electromagnetic ($\delta B_\perp$) gyrokinetic system requires a choice of formulation which numerically implies the use of implicit schemes or the 'cancellation problem' which grows with β and inversely with m_s and $k_\perp \rho_s$.

- The Hamiltonian approach, affected by the cancellation problem, may be most performant.

- We implement mitigation techniques to minimize this problem and test them with delta-*f* simulations of circular conventional and spherical tokamaks.

- Total-*f* XGC is uniquely placed to treat electromagnetic edge physics, e.g. ELM onset; almost all EM GK simulations so far are with delta-*f* codes.

Outline

- Introduction
- Stellarator XGC
- Explicit electromagnetic XGC
- Summary and outlook

Overview: Gyrokinetic code XGC for stellarators

- XGC is a gyrokinetic Particle-in-Cell (PIC) code for high fidelity modelling:
  - Gyrokinetic total-*f*
  - Electromagnetic ($\delta B_{\perp}$) (this talk!)
  - Non-linear multi-species collisions
  - Whole volume to first wall

- Stellarator version (this talk!) is currently:
  - Gyrokinetic delta-f
  - Electrostatic (EM ongoing…)
  - Collisionless
  - Whole volume to first wall (ongoing…)

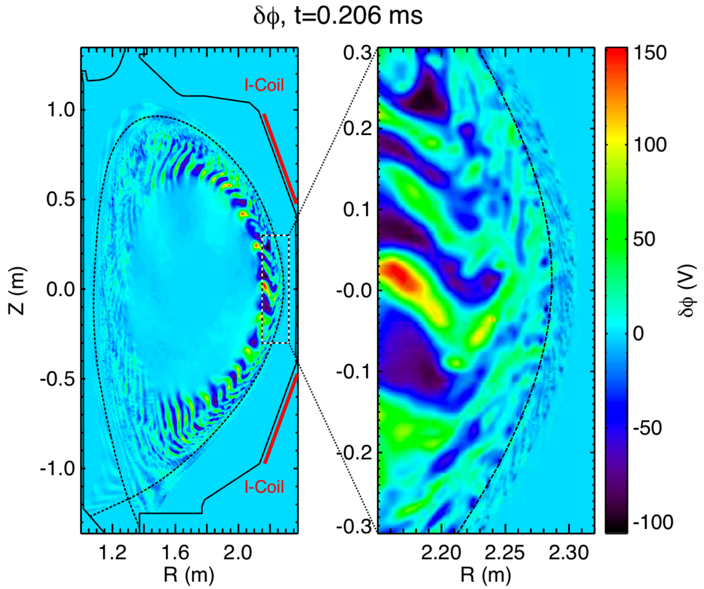

XGC simulation of electrostatic plasma turbulence with 3D magnetic perturbations (RMPs)

Ultimate goal: full high fidelity XGC capability with stellarator geometry

XGC for stellarators - Numerical implementation

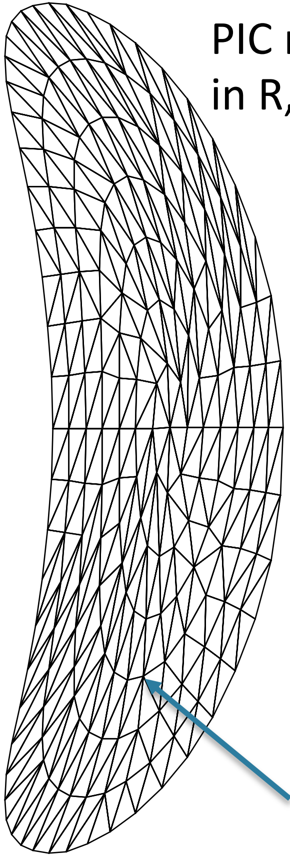

PIC markers pushed
in R, Z, φ

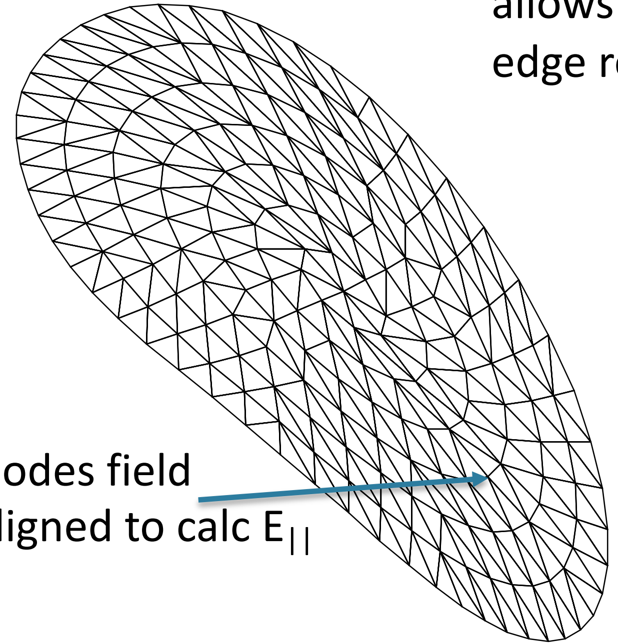

Unstructured mesh capability
allows smooth treatment of
edge region, with solver

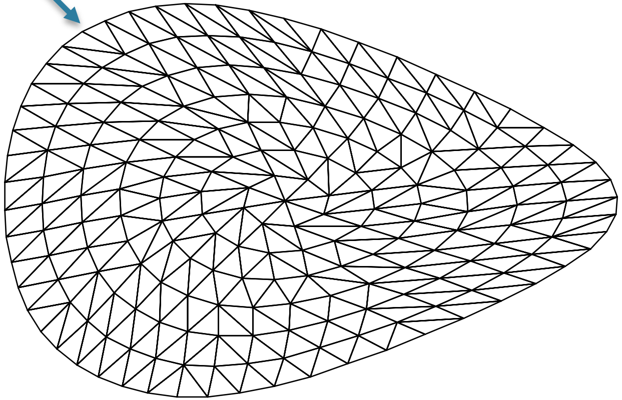

Nodes field
aligned to calc $E_{||}$

Potentials calc'd
on nodes

M. Cole *et al.*, Phys. Plasmas **26** 032506 (2019)
T. Moritaka *et al.,* Plasma 2 (2), 179-200, (2019)
M. Cole *et al.*, Phys. Plasmas **26** 082501 (2019)

Verification: Linear W7-X ITG benchmark

- Defined Wendelstein 7-X high mirror VMEC equilibrium (KJM)

  - R_0 = 5.5 m
  - a_0 = 0.505 m
  - B_0 = 2.41 T
  - $T_i(s = 0.5) = T_e(s = 0.5)$ = 1 keV
  - ITG driven unstable by quasi-local temperature gradient:

$$\frac{\mathrm{d}\ \ln T}{\mathrm{d}\ s} = -\sqrt{2}\left(\frac{1}{2} - \left|\, s - \frac{1}{2}\,\right|\right)\frac{a}{L_T}$$

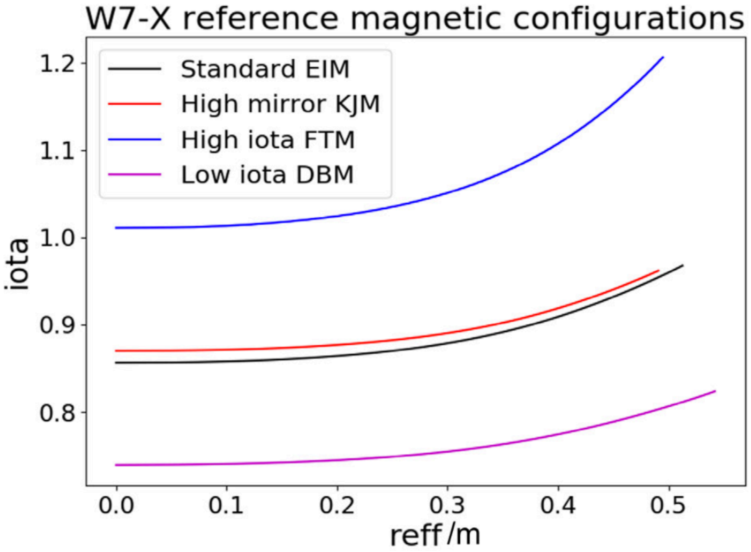

T. Klinger *et al.*, Nucl. Fusion **59** 112004 (2019)

- From experience, Wendelstein 7-X is the most challenging of the stellarator geometries numerically.

Verification: Linear W7-X ITG benchmark

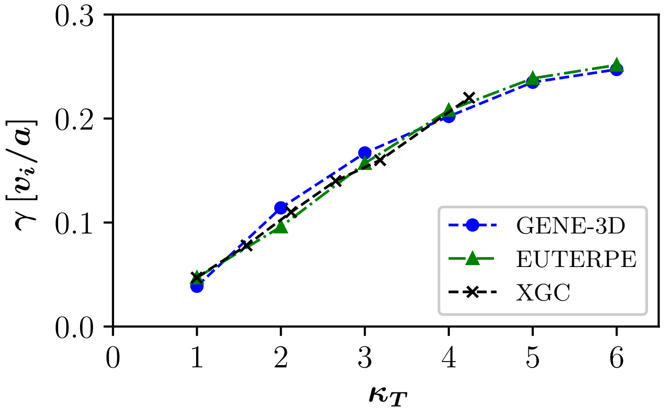

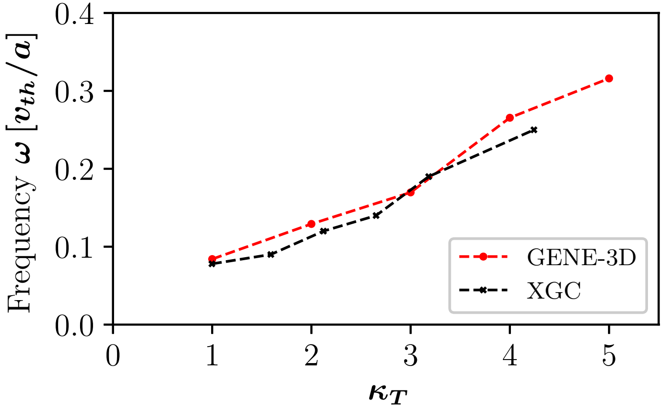

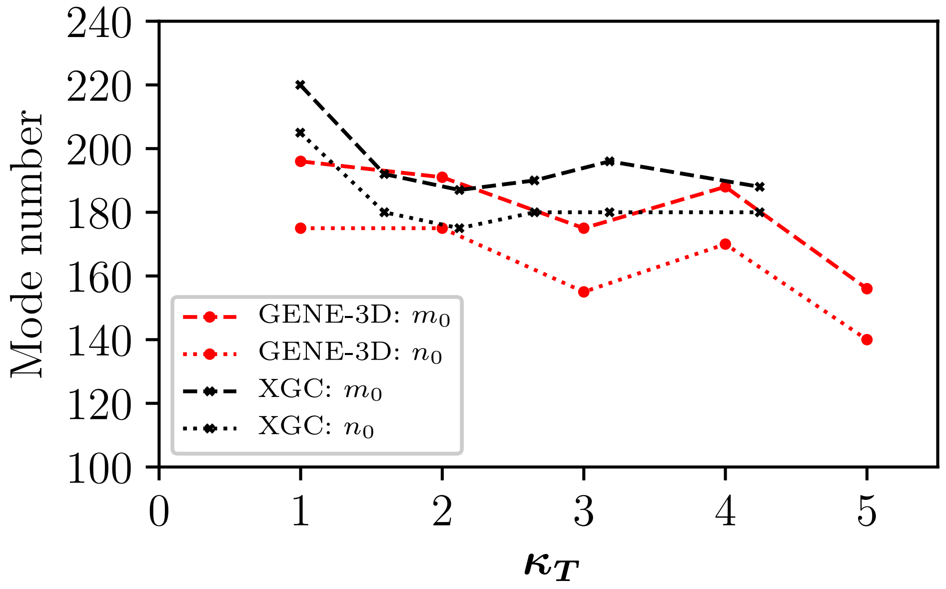

M. Cole *et al.*, Phys. Plasmas **26** 082501 (2019)
M. Maurer (GENE-3D), private communication

Verification: Linear W7-X ITG benchmark

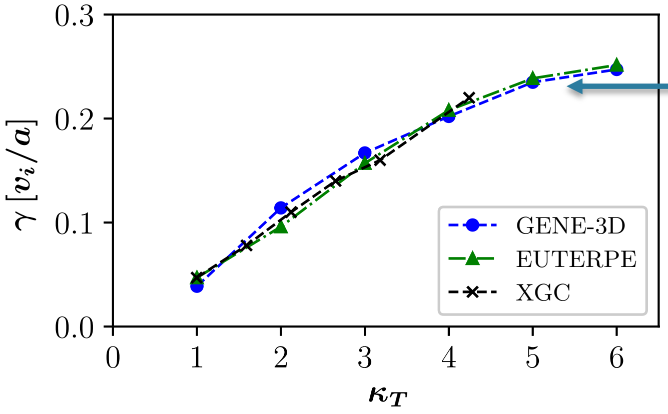

γ "rollover"

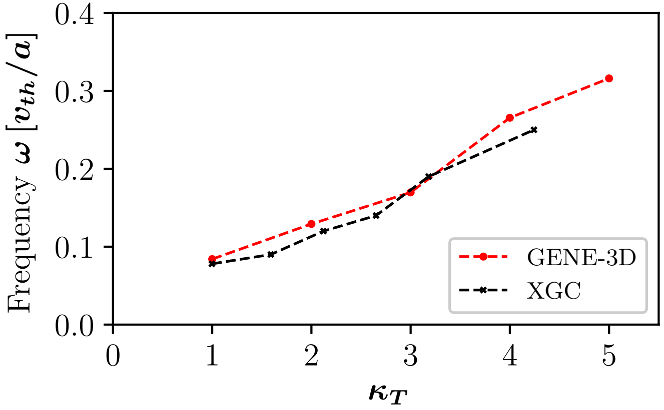

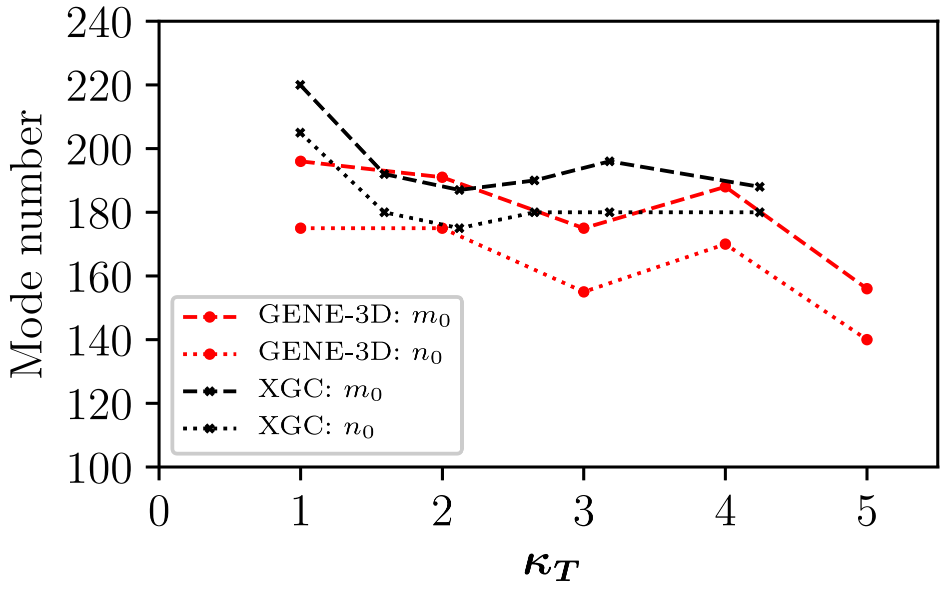

M. Cole *et al.*, Phys. Plasmas **26** 082501 (2019)
M. Maurer (GENE-3D), private communication

W7-X and QUASAR comparison

- Original EUTERPE case included Wendelstein 7-X and LHD.

- Extend this to PPPL's QUASAR/NCSX, keeping T, n profiles the same.

Negative iota shear (positive q shear) case used – lowest turbulent transport with local GENE simulations.

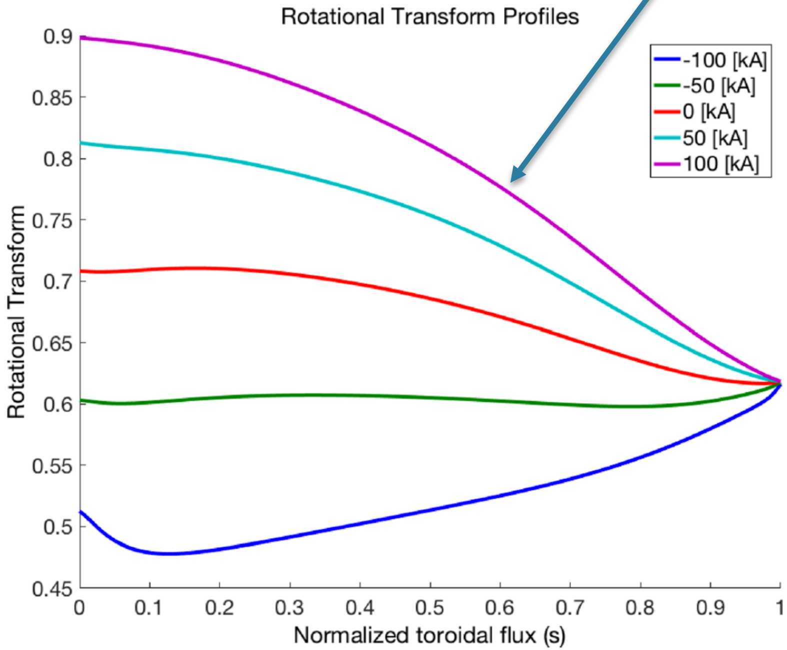

S. Lazerson *et al.*, Phys. Plasmas **26** 022509 (2019)

W7-X and QUASAR comparison

- Original EUTERPE case included Wendelstein 7-X and LHD.
- Extend this to PPPL's QUASAR/NCSX, keeping T, n profiles the same.
- Normalised growth rates are almost the same for all three devices (see right, LHD growth rates followed W7-X).

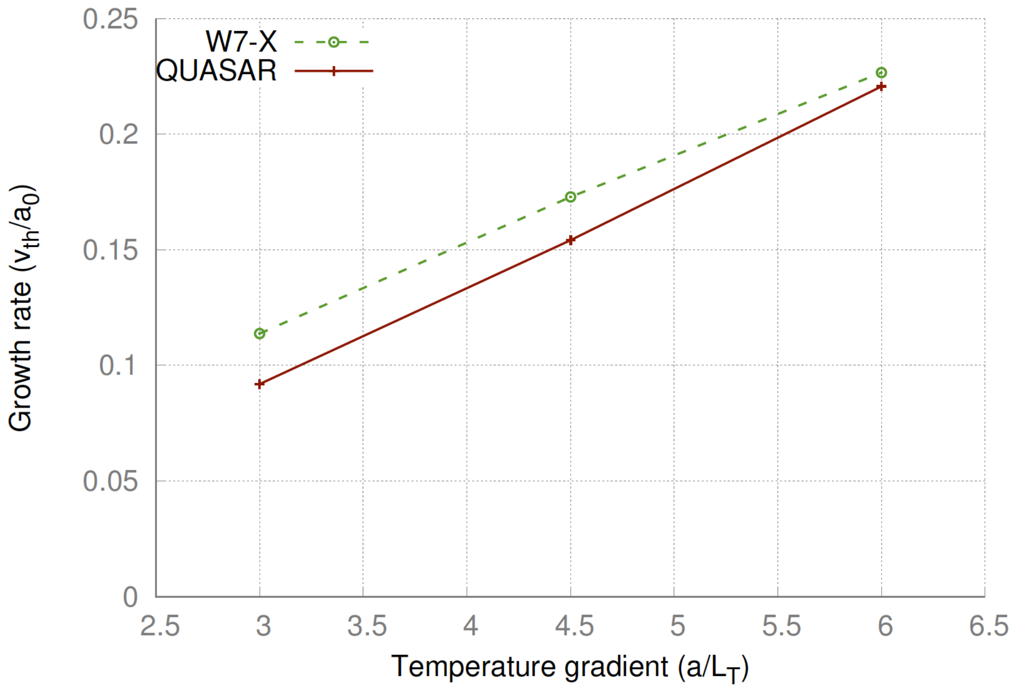

M. Cole *et al.*, Phys. Plasmas, under review (2020)

W7-X and QUASAR comparison – mode numbers

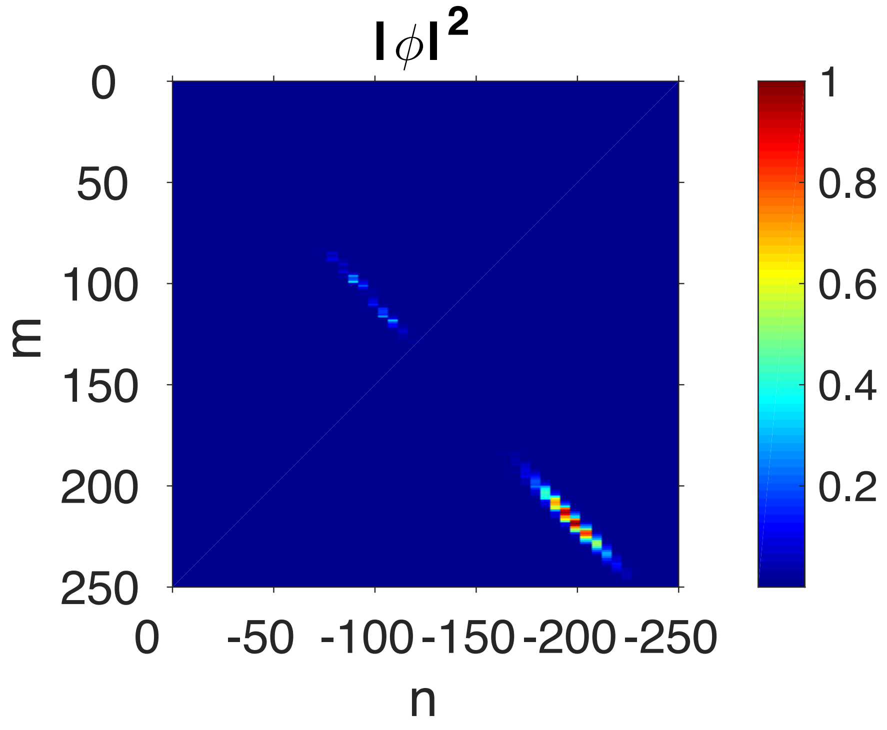

W7-X

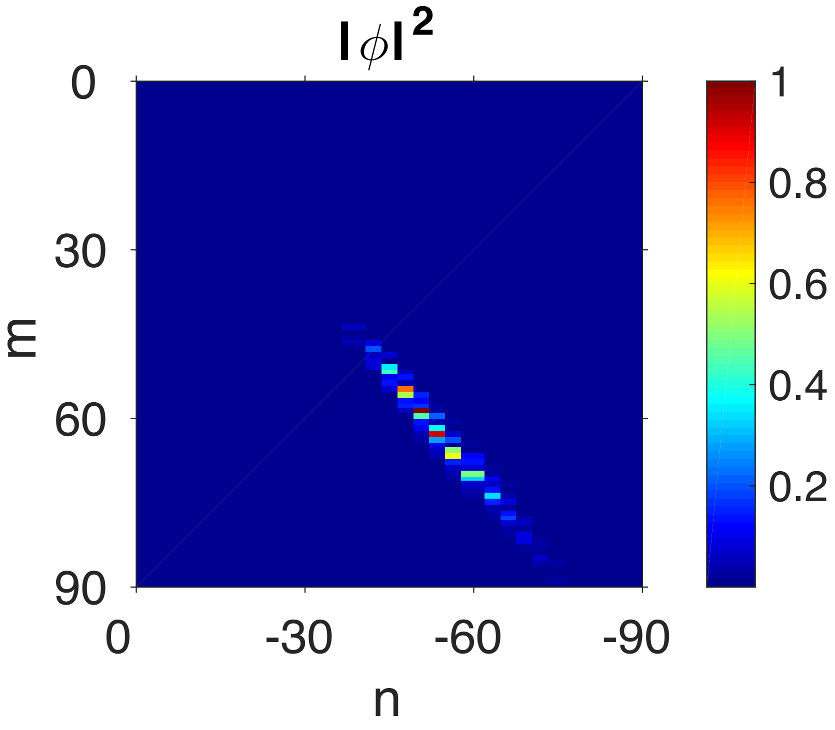

QUASAR

M. Cole *et al.*, Phys. Plasmas, under review (2020)

W7-X and QUASAR: mode structure differences

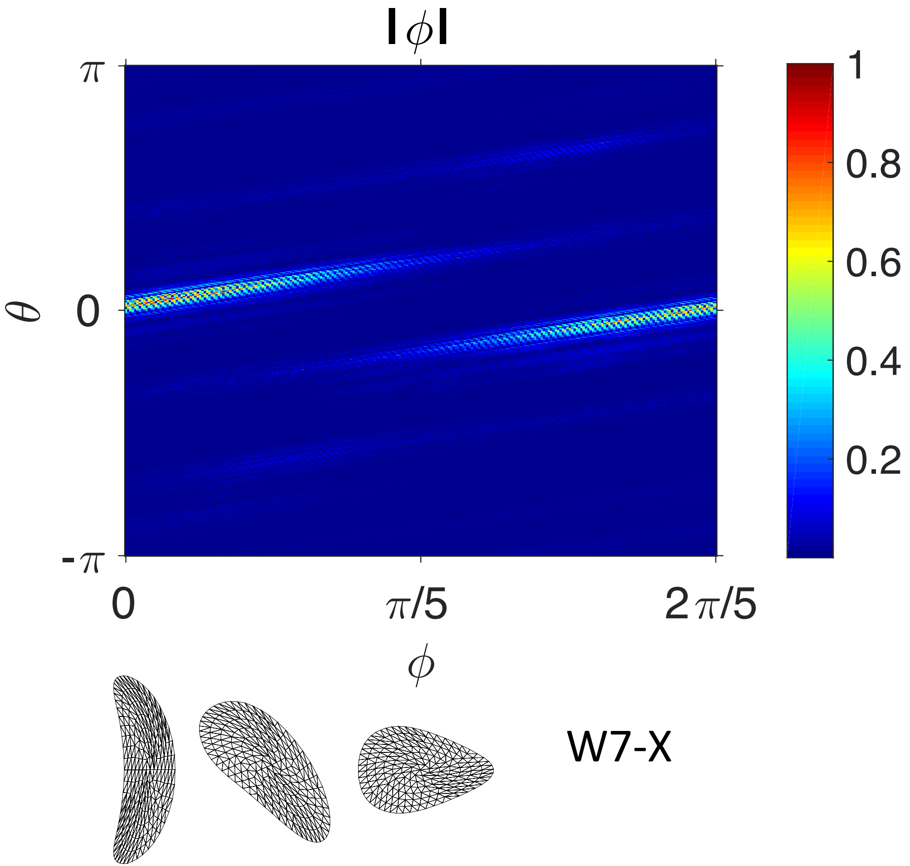

W7-X

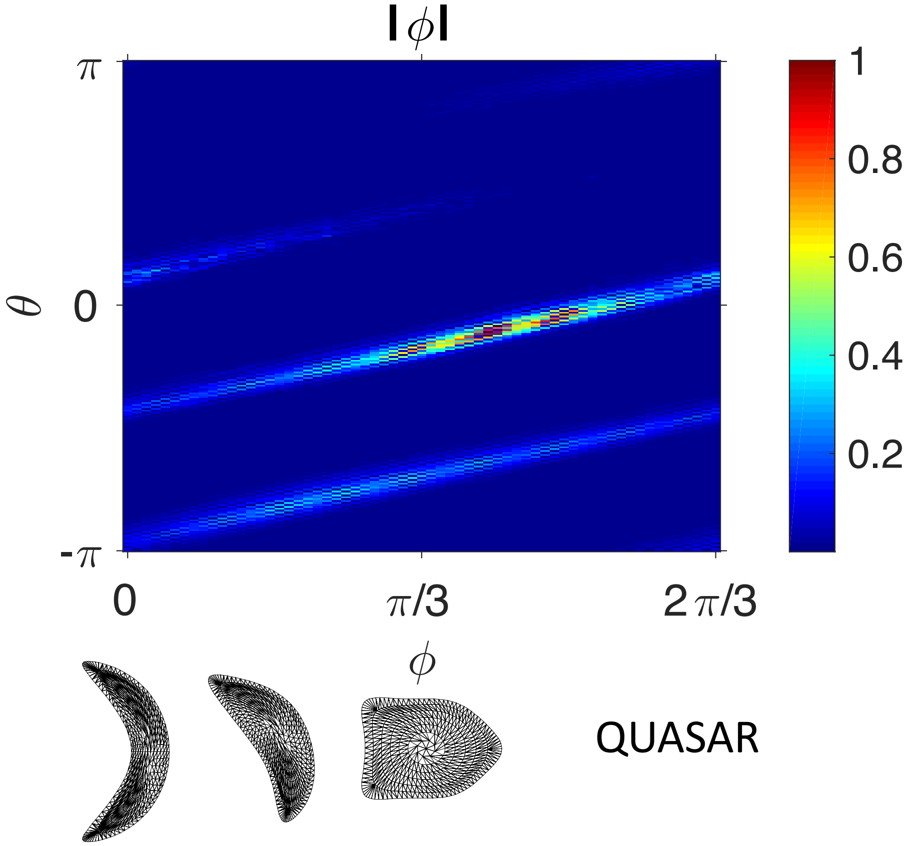

QUASAR

M. Cole *et al.*, Phys. Plasmas, under review (2020)

W7-X and QUASAR comparison – mode structures

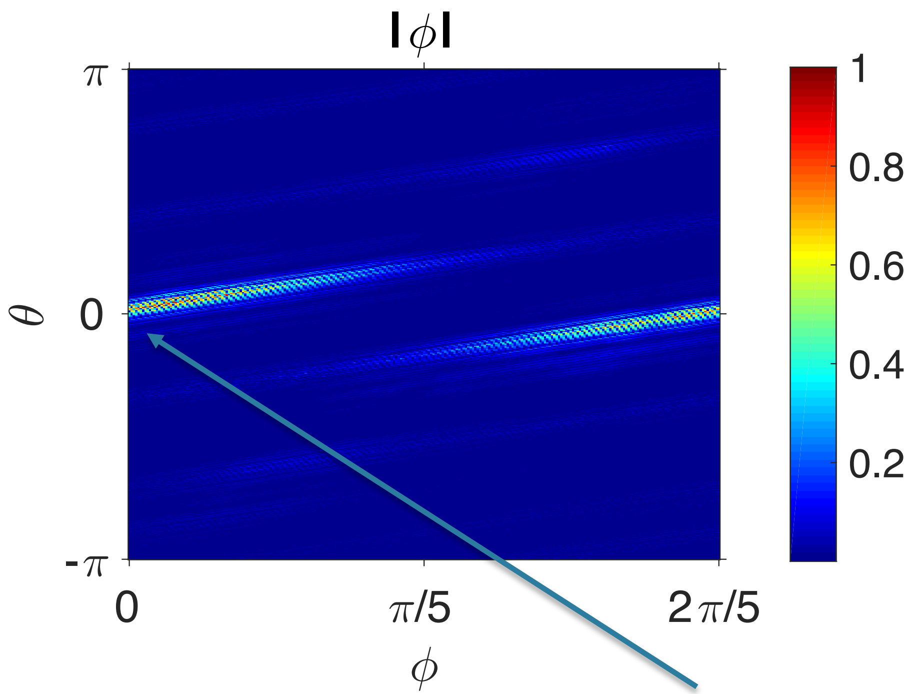

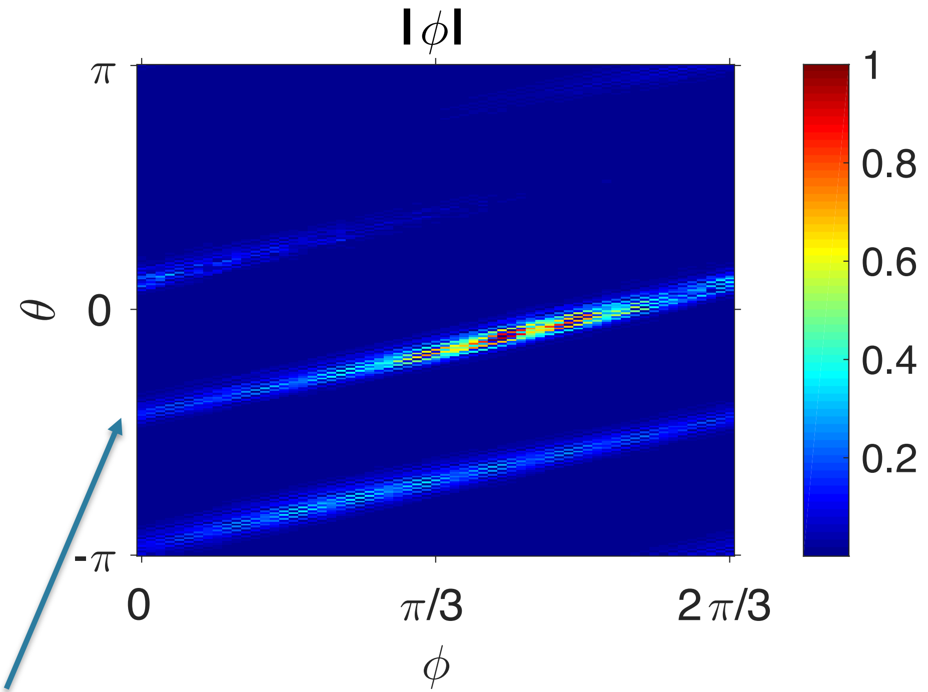

Poloidal shift predicted theoretically due to radial shear in iota, mode frequency; stronger at higher growth rate.

Y. Camenen *et al.*, Nucl. Fusion **51** 073039 (2011)

$$\theta_0|_{\gamma_{\max}} = -\mathrm{sign}(\hat{s}\omega_r')\left[\frac{\omega_r'}{2k_\theta\gamma_0\hat{s}}\right]^{\frac{1}{3}}$$

M. Cole *et al.*, Phys. Plasmas, under review (2020)

Global nonlinear verification: XGC1 tokamak benchmark

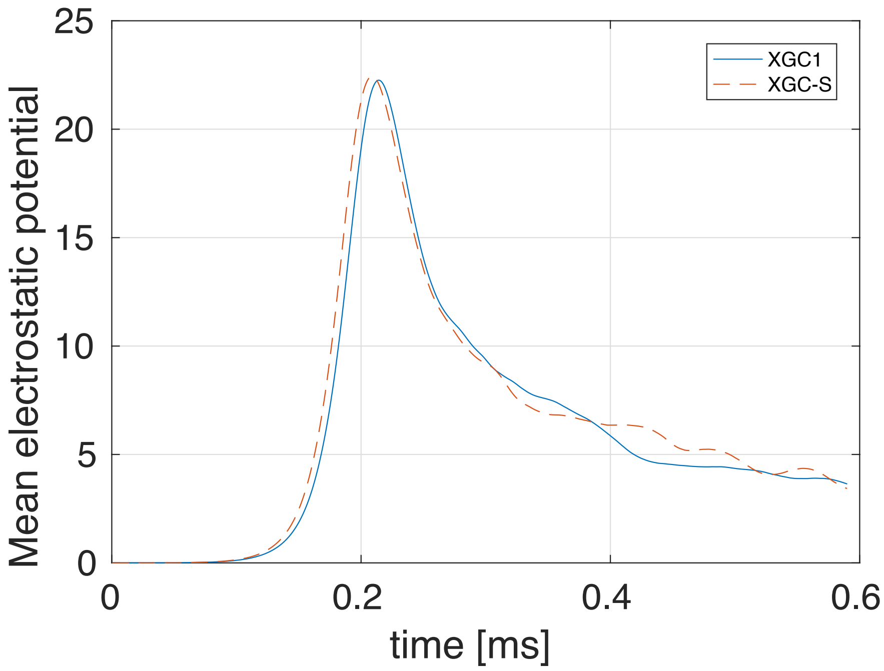

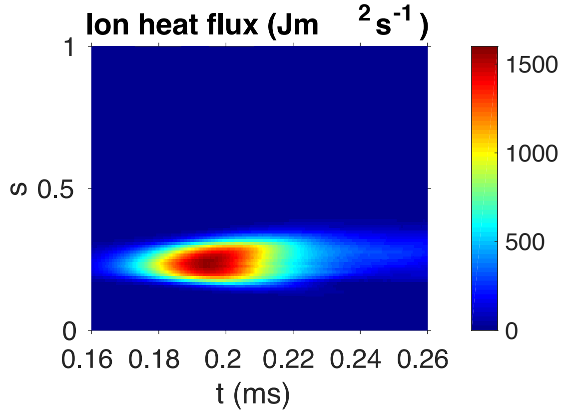

XGC1

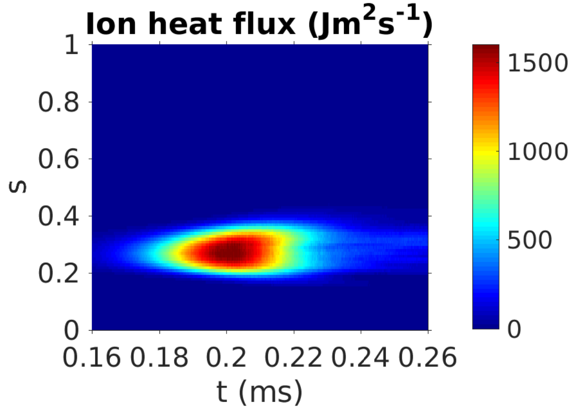

XGC-S

M. Cole *et al.*, Phys. Plasmas, under review (2020)

Global nonlinear ITG in QUASAR: heat flux

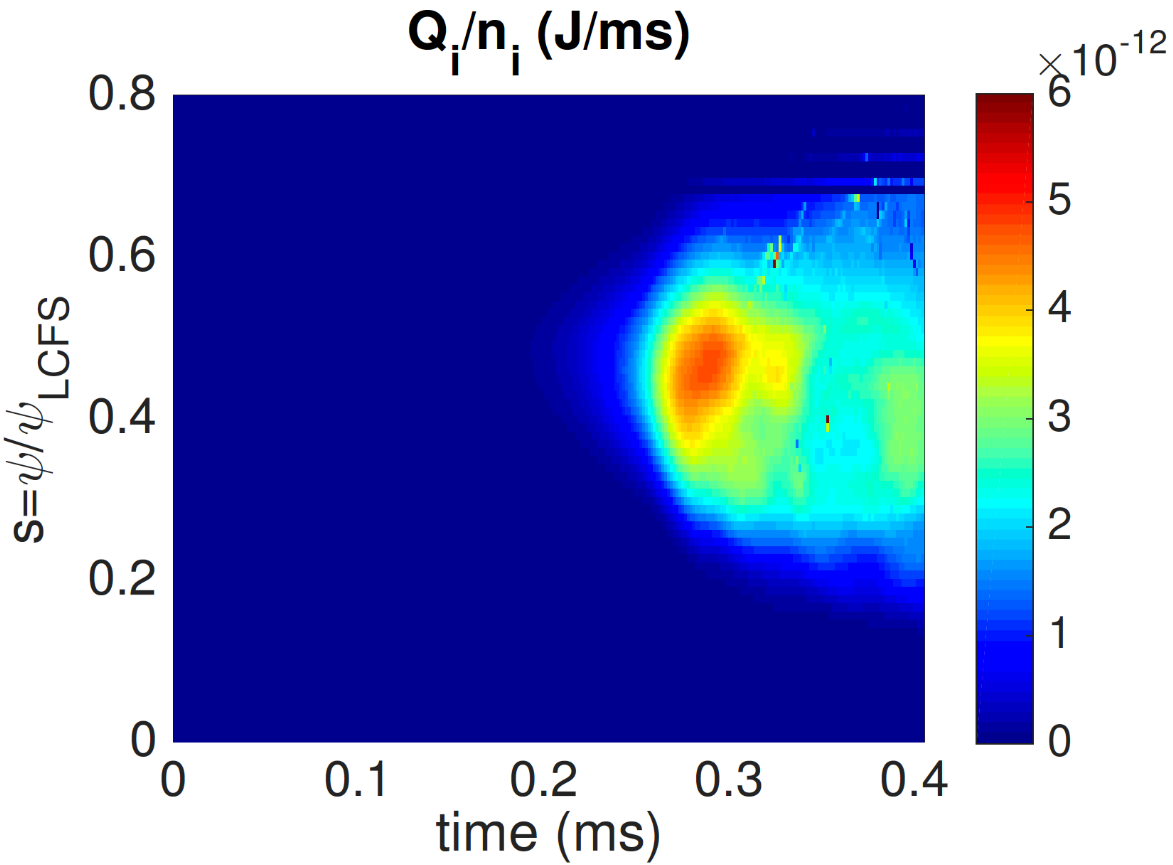

t = 0.15ms

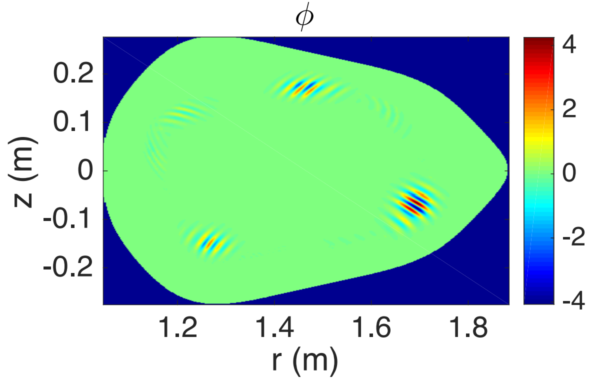

t = 0.3ms

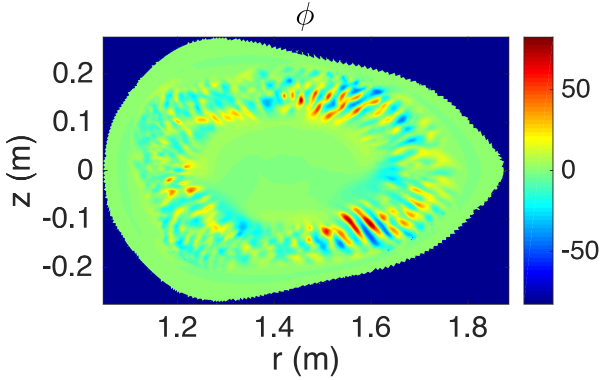

M. Cole *et al.*, Phys. Plasmas, under review (2020)

Global nonlinear ITG in QUASAR: heat flux

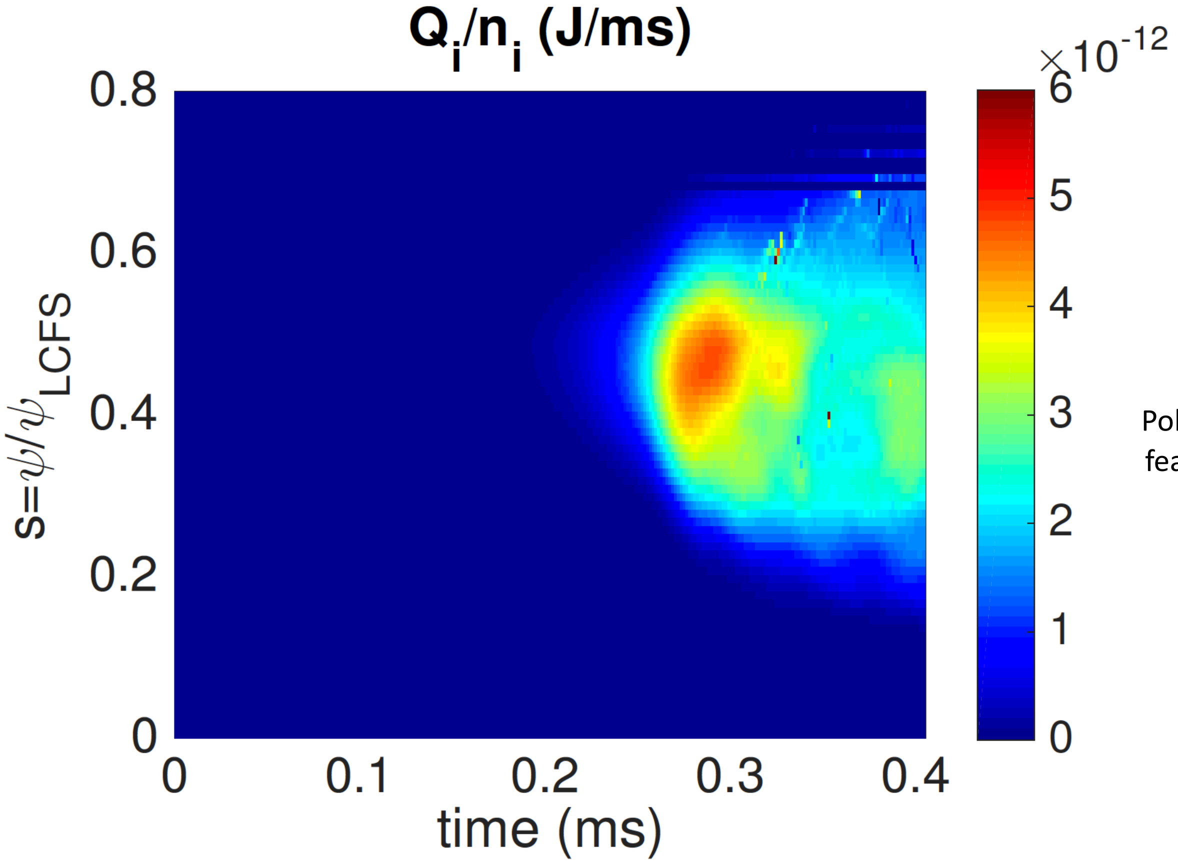

t = 0.15ms

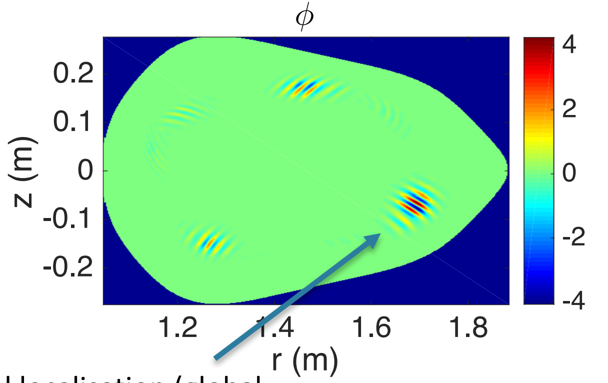

Poloidal localisation (global feature) weakened at peak

t = 0.3ms

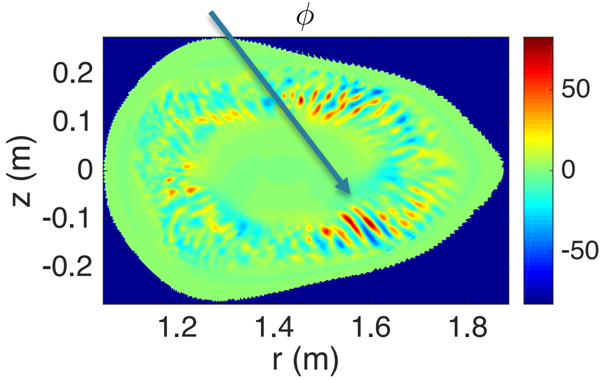

M. Cole *et al.*, Phys. Plasmas, under review (2020)

Progress towards a whole volume capability

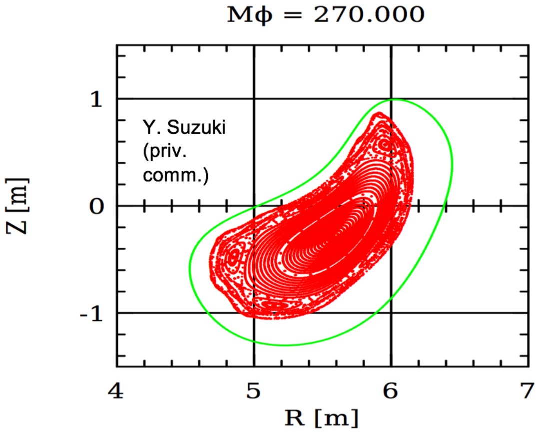

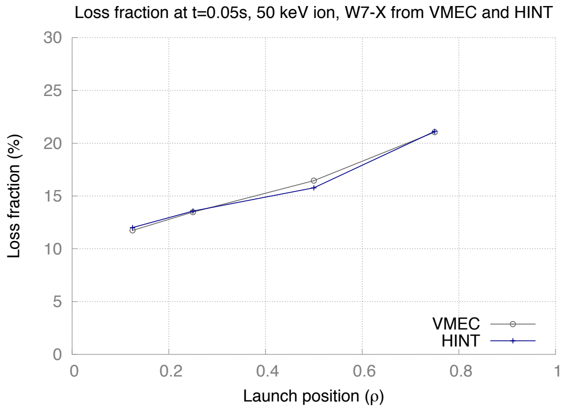

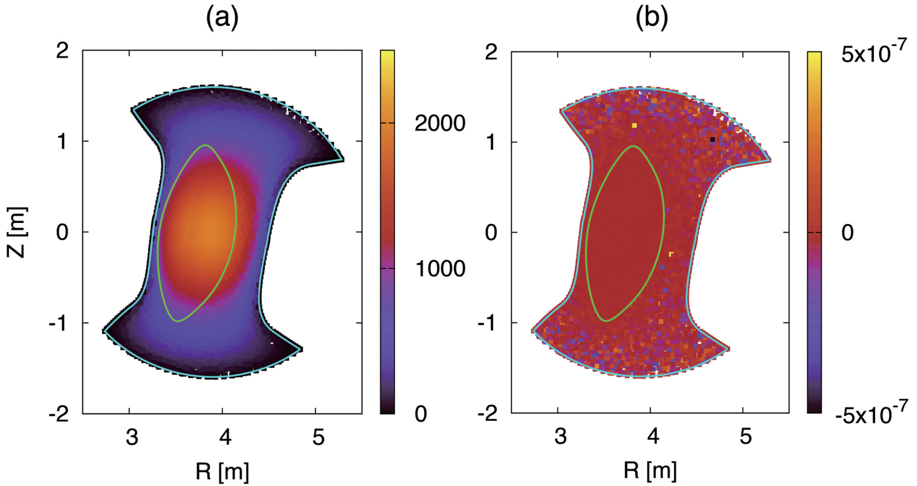

T. Moritaka *et al.*, Plasma 2 (2), 179-200, (2019)

- Poisson solver test with constant charge distribution (above left – electrostatic potential; right – relative error to analytical solution).
- HINT3D equilibrium test with islands, stochastic regions (left, core).

Outline

- Introduction
- Stellarator XGC
- Explicit electromagnetic XGC
- Summary and outlook

Electromagnetic gyrokinetics: cancellation problem

Symplectic formulation ($v_{||}$)

$$\dot{\vec{R}} = v_\parallel \vec{\tilde{b}}^* + \frac{1}{q\tilde{B}_\parallel^*}\vec{b} \times \left[\mu \nabla B + q\left(\nabla\langle\phi\rangle + \frac{\partial\langle A_\parallel\rangle}{\partial t}\vec{b}\right)\right]$$

- No cancellation problem.
- Implicit methods required (for XGC: B. Sturdevant, L. Chacón, M. Adams)

Hamiltonian formulation ($p_{||}$)

$$p_{||} = mv_{||} + qA_{||}$$

$$\left(\sum_{s=i,e,f}\frac{\hat{\beta}_s}{\rho_s^2} - \nabla_\perp^2\right)A_\parallel = \mu_0 \sum_{s=i,e,f}\bar{j}_{\parallel 1s}$$

- Cancellation problem scales as:

$$\delta A_\parallel \sim \beta/(k_\perp^2\rho_e^2)$$

- Explicit schemes possible (RK4 etc.).

Electromagnetic gyrokinetics: mixed formulation

- Combine Hamiltonian and symplectic formulations in derivation of GK system:

$$\sum_{s=\mathrm{i,e,f}} \frac{\beta_s}{\rho_s^2} \langle \bar{A}_\parallel^{(\mathrm{h})} \rangle_s - \nabla_\perp^2 A_\parallel^{(\mathrm{h})} = \mu_0 \sum_{s=\mathrm{i,e,f}} j_{\parallel 1s} + \nabla_\perp^2 A_\parallel^{(\mathrm{s})}$$

- Introduces new degree of freedom:

$$\frac{\partial}{\partial t} A_\parallel^{(\mathrm{s})} + \boldsymbol{b} \cdot \nabla \phi = 0.$$

- Cancellation problem occurs only in $A_{||}^{(h)}$: reset phase space at each timestep (right).

$p_{||} = mv_{||} + qA_{||}^{(h)}$

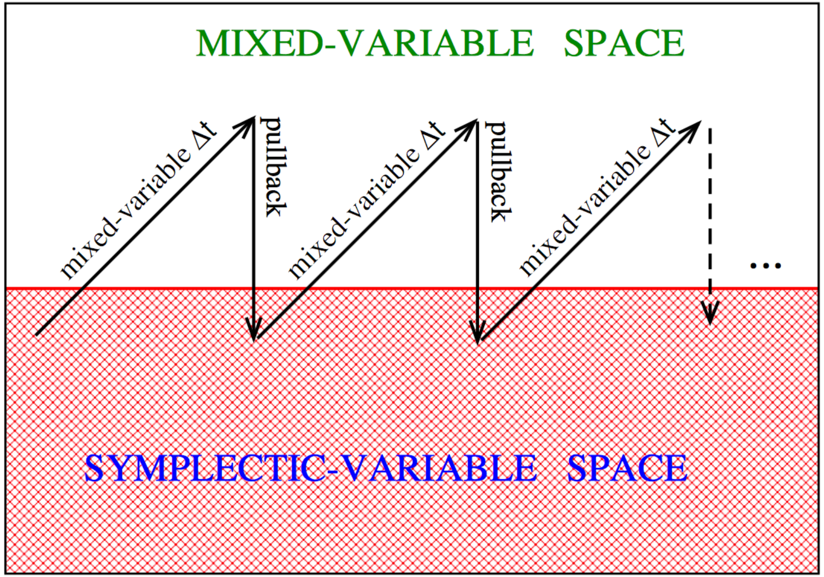

A. Mishchenko, M. Cole, R. Kleiber and A. Könies, Phys. Plasmas **21** 052113 (2014)
A. Mishchenko, A. Könies, R. Kleiber and M. Cole, Phys. Plasmas **21** 092110 (2014)

ITG-KBM transition benchmark

- Hamiltonian equations alone (m_i/m_e=100) -> realistic electron mass with mitigation techniques.

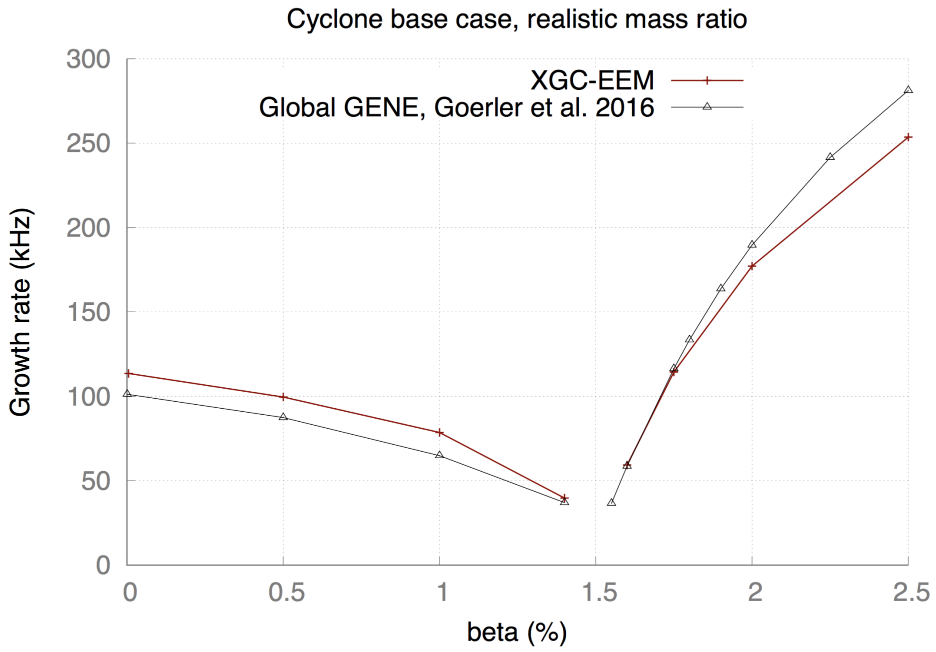

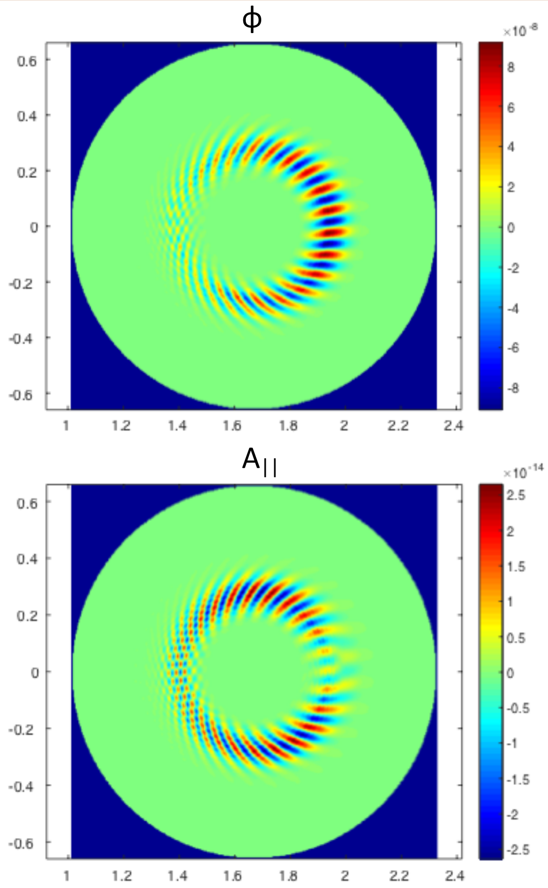

M. Cole *et al.*, in preparation

Electromagnetics in spherical tokamaks

- Predicting the KBM transition point is a key research question for spherical tokamaks.

- XGC NSTX-like case, with mitigation techniques:
  - $R_0 = 0.85$ m
  - $a_0 = 0.67$ m
  - $B_0 = 0.45$ T
  - $q_0 = 1.21$, $q_{95} = 3.86$
  - $\kappa = 2.2$
  - $\beta_{s=0.25} = 2.34\%$

- $\gamma = 54$ kHz (159 kHz without elongation)

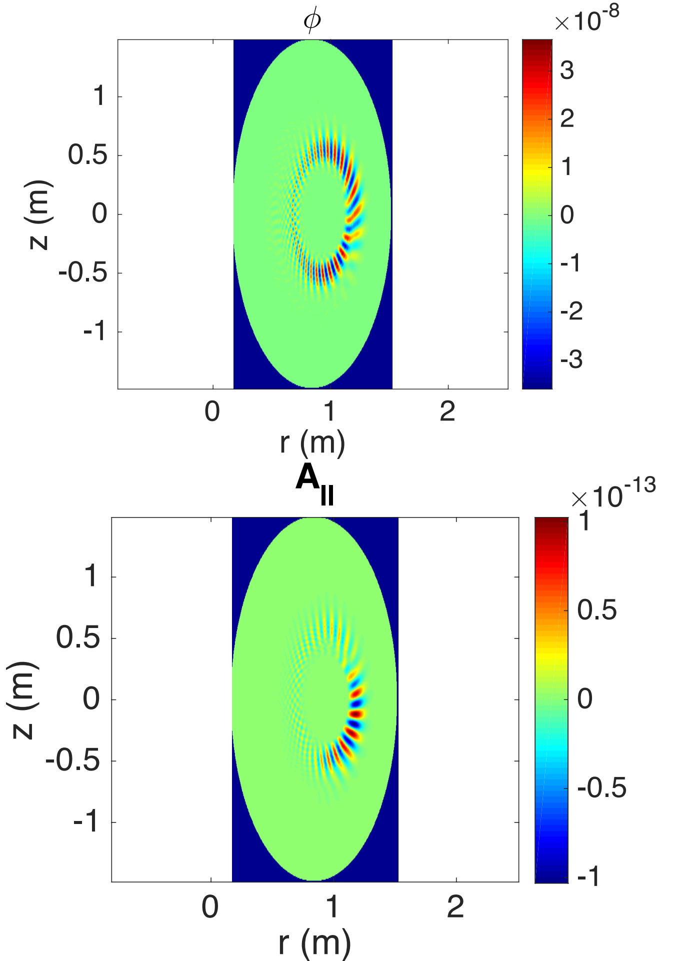

Outline

- Introduction
- Stellarator XGC
- Explicit electromagnetic XGC
- Summary and outlook

Summary

- Delta-*f* electrostatic core physics with XGC-S has been successfully benchmarked with EUTERPE, GENE-3D.

- First physics studies in NCSX/QUASAR geometry have been performed into the turbulent phase.

- State-of-the-art explicit electromagnetic techniques have been implemented in XGC.

- Proof of principle KBM simulations in geometry similar to NSTX have been performed successfully.

Outlook

- KBMs may be key to optimized stellarator confinement – combine stellarator and EM developments (total-*f*?)
- Whole volume stellarator version with islands and stochastic regions under development.
- Comparison to experiment planned with PPPL powder dropper on LHD.
- KBM modelling in spherical tokamaks such as NSTX-U – KBM threshold is a key physics question for STs.
- Model MTMs in NSTX-U to understand *e*- heat flux.
- High fidelity turbulence modelling can be used to develop reduced models for stellarators (machine learning?).

W7-X (linear GENE flux tube)

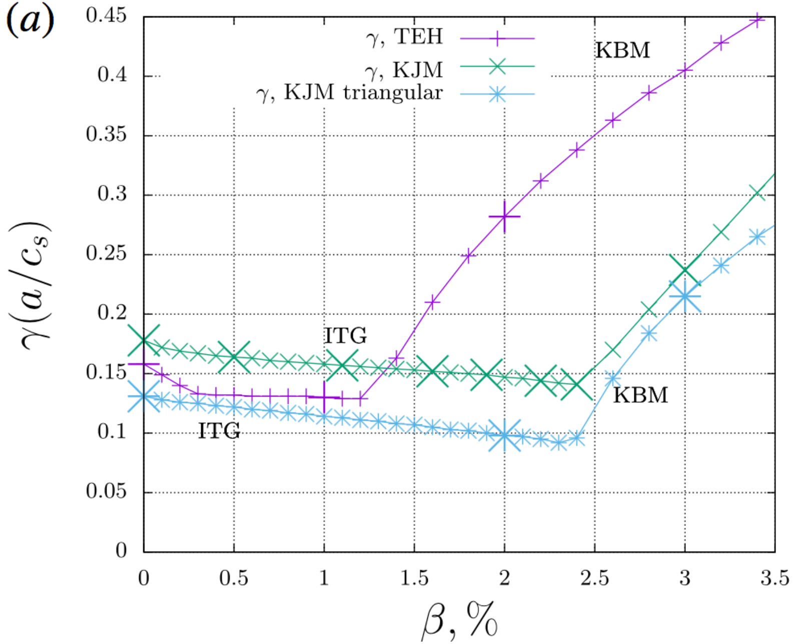

K. Aleynikova and A. Zocco, J. Plasma Phys. **84** 0602 (2018)

Backup: electrostatic GK equations

Without sources, sinks, or collisions and neglecting any background electric field, ϕ_0, the perturbed distribution function evolution equation[30] solved by XGC-S is

$$\frac{\partial\,\delta f}{\partial t} + \dot{\vec{X}} \cdot \frac{\partial\,\delta f}{\partial \vec{X}} + \dot{v}_{\parallel} \frac{\partial\,\delta f}{\partial v_{\parallel}} = -\dot{\vec{X}}_1 \cdot \frac{\partial f_0}{\partial \vec{X}} - \dot{v}_{\parallel 1} \frac{\partial f_0}{\partial v_{\parallel}} \tag{1}$$

where $\vec{X}$ is the gyrocentre position,

$$\dot{\vec{X}} = \frac{1}{G}\left[v_{\parallel}\vec{b} + \frac{m v_{\parallel}^2}{qB}\nabla \times \vec{b} + \frac{1}{qB^2}\vec{B} \times \left(\mu \nabla B + q\nabla\langle\phi\rangle\right)\right], \tag{2}$$

$v_{\parallel}$ is the gyrocentre velocity,

$$\dot{v}_{\parallel} = -\frac{1}{mG}\left(\vec{b} + \frac{m v_{\parallel}}{qB}\nabla \times \vec{b}\right) \cdot \left(\mu \nabla B + q\nabla\langle\phi\rangle\right) \tag{3}$$

and

$$G = 1 + \frac{m v_{\parallel}}{qB}\vec{b} \cdot \left(\nabla \times \vec{b}\right), \tag{4}$$